

Molecular Interactions of Ether-Linked Phospholipids<sup>†</sup>

Frederick S. Hing and G. Graham Shipley\*

Departments of Biophysics and Biochemistry, Boston University School of Medicine, Boston, Massachusetts 02118

Received February 14, 1995; Revised Manuscript Received July 17, 1995<sup>®</sup>

**ABSTRACT:** Earlier studies have shown that ether phospholipids display phase-forming properties distinct from those of their ester phospholipid counterparts. Dihexadecylphosphatidylcholine (DHPC) forms an interdigitated bilayer when fully hydrated, and dihexadecylphosphatidylethanolamine (DHPE) is observed in the inverted hexagonal phase ( $H_{II}$ ) at elevated temperatures. In contrast, the acyl lipid analogues display these phases only under more extreme conditions. In the present study, we examine fully hydrated mixtures of DHPC and DHPE by X-ray diffraction and differential scanning calorimetry and describe the temperature–composition phase diagram for the binary phospholipid system, DHPC/DHPE. Addition of 7 mol % DHPE to DHPC abolishes the ability of DHPC to form an interdigitated bilayer gel phase ( $L_{\beta I}$ ), whereas 10 mol % DHPC destabilizes the  $H_{II}$  phase favored by DHPE by elevating (to  $>100$  °C) or removing the  $L_{\alpha} \rightarrow H_{II}$  transition. Evidence for bilayer gel phase separation occurring in DHPC/DHPE mixtures is obtained. In conclusion, it is found that small amounts of the appropriate phospholipid can seriously compromise the formation of the  $L_{\beta I}$  and  $H_{II}$  phases.

The lipid bilayer matrix of plasma membranes is built by using a complex mixture of different phospholipids, sphingomyelins, glycosphingolipids, and cholesterol. These lipids assemble to form the stable lipid bilayer matrix into which specific functional membrane proteins (channels, receptors, enzymes, etc.) are incorporated. Individual lipids such as phosphatidylcholine (PC),<sup>1</sup> sphingomyelin, cerebroside, and digalactosyl diglyceride (DGDG) spontaneously assemble to form bilayers, whereas others, including phosphatidylethanolamine (PE) and monogalactosyl diglyceride (MGDG), prefer to form nonbilayer structures such as the hexagonal  $H_{II}$  phase. The molecular basis underlying lipid phase formation has been discussed in terms of shape [for a review, see Israelachvili et al. (1980)] or intrinsic curvature (Gruner, 1985) arguments. Recently, it has been shown that in some bacterial membranes the ratio of bilayer-forming and hexagonal-forming lipids is regulated in some way. For example, in *Acholeplasma laidlawii* the DGDG/MGDG ratio responds to manipulations of the membrane fatty acid composition (Wieslander et al., 1980, 1981a,b); a similar effect has been noted in *Clostridium butyricum* where the ratio of bilayer-forming glycerol acetal PE to hexagonal-preferring PE again responds to alterations in fatty acid composition (Goldfine et al., 1987). It is not clear whether the structural characteristics of individual lipid components are exploited in regions of membranes responsible for specific functions (e.g.,  $H_{II}$ -forming lipids in lipid–protein interactions or at sites of membrane fusion) or whether the

combination of lipids provides some optimal overall structural property.

Our studies have focused on the structures and properties of different membrane lipids. For example, we have defined the effects of variations in (i) polar head group structure [PE (Chapman et al., 1966; Hitchcock et al., 1974), methylated PEs (Mulukutla & Shipley, 1984), PC (Janiak et al., 1976, 1979; Ruocco et al., 1982a,b), phosphatidylserine (Hauser et al., 1982), etc.] and (ii) hydrocarbon chain length, unsaturation, and distribution [for PC, see Mattai et al. (1987); Shah et al., 1990, 1994]. These studies, together with those of other workers in this field, clearly show that variations in either polar group or chain moieties lead to alterations in lipid structure and properties. However, recent studies suggest that in phospholipids alterations in the mode of chain linkage to the glycerol backbone also play a role. For example, for PC, substitution of ether linkages (alkyl) for ester (acyl) linkages for the attachment of chains at the sn-1 and sn-2 positions alters both the structural and thermotropic properties. The usual bilayer gel phase of the ester-linked dipalmitoyl-PC (DPPC) is replaced by a chain-interdigitated “monolayer” structure in its ether-linked analogue, dihexadecyl-PC (DHPC) (Ruocco et al., 1985; Kim et al., 1987a; Laggner et al., 1987). Studies of the mixed ether–ester compound, 1-hexadecyl-2-palmitoyl-PC (HPPC), demonstrate that substitution at only the sn-1 position is sufficient to permit the formation of the interdigitated monolayer gel phase (Haas et al., 1990). In mixed DPPC/DHPC systems, both types of gel phase are formed (bilayer or interdigitated monolayer), depending on the composition (Kim et al., 1987b; Lohner et al., 1987).

In both animal and bacterial membranes, significant amounts of PE with chains attached at the sn-1 position by ether (or vinyl ether, i.e., plasmalogen) linkages are found, and minor amounts of dialkyl lipids are found in some tissues (Snyder, 1991). Substitution of an ether for an ester linkage lowers the bilayer ( $L_{\alpha}$ )  $\rightarrow H_{II}$  transition temperature, but has little effect on the lower bilayer gel  $\rightarrow L_{\alpha}$  transition (Boggs et al., 1981). In addition, Seddon and co-workers have

<sup>†</sup> This work was supported by Research Grant HL-26335 and Training Grant HL-07429 (F.S.H.) from the National Institutes of Health.

\* Author to whom correspondence should be addressed.

<sup>®</sup> Abstract published in *Advance ACS Abstracts*, September 1, 1995.

<sup>1</sup> Abbreviations: PE, phosphatidylethanolamine; PC, phosphatidylcholine; DHPE, 1,2-dihexadecyl-sn-glycero-3-phosphoethanolamine; DHPC, 1,2-dihexadecyl-sn-glycero-3-phosphocholine; DPPC, 1,2-dipalmitoyl-sn-glycero-3-phosphocholine; HPPC, 1-hexadecyl-2-palmitoyl-sn-glycero-3-phosphocholine; DPPE, 1,2-dipalmitoyl-sn-glycero-3-phosphoethanolamine; DSC, differential scanning calorimetry; DGDG, digalactosyl diglyceride; MGDG, monogalactosyl diglyceride.

defined the phase behavior of a series of ester- and ether-linked PEs (Seddon et al., 1983). In an earlier study (Hing et al., 1991), we defined the hydration dependence of the structure and properties of one member of the ether-linked series, dihexadecyl-PE (DHPE) and its interactions with its ester-linked analogue, dipalmitoyl-PE (DPPE). We now report on the interactions of the two ether-linked phospholipids, DHPE and DHPC.

## MATERIALS AND METHODS

DHPC (Fluka) and DHPE (Berchtold, Berne, Switzerland) were shown to be >98% pure by thin-layer chromatography using the solvent system chloroform/methanol/water (65/35/4, v/v/v) and were utilized without further purification. DHPC/DHPE mixtures of known molar ratio were prepared by weighing appropriate amounts of each lipid into a small vial and dissolving them in a chloroform/methanol solution (2/1, v/v). The solvent was blown off with a gentle stream of nitrogen, and the lipid mixture was placed overnight under high vacuum.

Samples for differential scanning calorimetry (DSC) were prepared by weighing the lipid mixture into stainless steel pans. Sufficient distilled, deionized water was added with a syringe to fully hydrate the sample (70 wt % H<sub>2</sub>O), and the pans were sealed and weighed again to accurately determine water content. DSC was performed on both Perkin-Elmer DSC-2 and DSC-7 calorimeters (Norwalk, CT). Heating and cooling rates of 5 °C/min were used over the temperature range of 0–99 °C. Samples were heated and cooled repeatedly to ensure equilibration of the lipid and water. The peak maxima,  $T_m$ , as well as the onset and completion temperatures of the transitions were determined. A gallium standard was used for calibration. Additional DSC experiments were performed on DHPE/DHPC mixtures with a Microcal-2 calorimeter (Amherst, MA). Aqueous dispersions of lipid (1.5 mg/mL) were examined at heating rates of 90 °C/h.

X-ray diffraction samples were prepared by weighing the appropriate lipid mixture into a 1.0 mm (i.d.) quartz capillary. Distilled, deionized water was added to fully hydrate the lipid (70 wt % H<sub>2</sub>O). Capillaries were then sealed and heated above the chain-melting transition temperature while simultaneously centrifuging in a clinical centrifuge at high speed. Samples were inverted and centrifuged back and forth in the capillary several times in order to achieve homogeneous mixing. X-ray diffraction patterns were recorded on photographic film using nickel-filtered Cu K $\alpha$  radiation ( $\lambda = 1.5418$  Å) from an Elliott GX-6 rotating-anode generator (Elliott Automation, Borehamwood, U.K.) and focused with either double-mirror (Franks, 1958) or toroidal (Elliott, 1965) optics. Microdensitometry was performed on a Joyce Loebel (Gateshead, U.K.) Model III-CS scanning microdensitometer.

## RESULTS

**DSC of Fully Hydrated DHPE/DHPC Mixtures.** DSC heating curves of fully hydrated mixtures of DHPE and DHPC are shown in Figure 1. Pure DHPC in excess water exhibited two reversible, endothermic transitions upon heating. A low-enthalpy pretransition occurred at  $T_m = 36$  °C ( $\Delta H = 6.6$  J/g), and a large-enthalpy main transition took place at  $T_m = 46$  °C ( $\Delta H = 46.0$  J/g). Addition of 7 mol % DHPE to DHPC appeared to abolish the small pretransition,

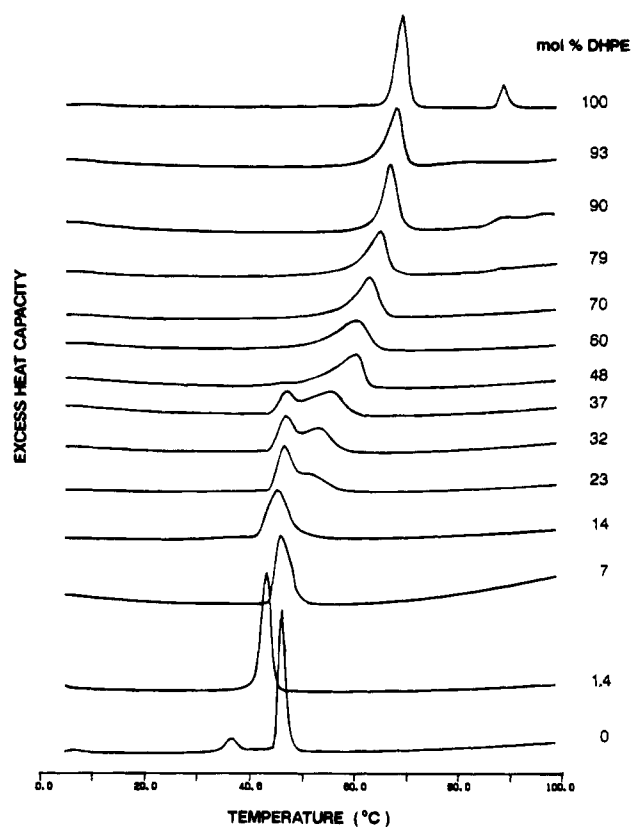


FIGURE 1: DSC heating curves of fully hydrated (70 wt % H<sub>2</sub>O) lipid mixtures containing various mol % of DHPE and DHPC (heating rate, 5 °C/min).

and only a single asymmetric peak at 46 °C was seen. Continued addition of DHPE resulted in a slight increase in the peak temperature as well as a broadening of the transition. With increasing contents of DHPE, the DSC heating scans became increasingly complex, and two maxima (at 47 and 53 °C) in the heat capacity curves were obvious at 32 mol % DHPE. Above approximately 40 mol % DHPE, only the higher temperature peak was observed along with a low-temperature shoulder. This peak moved to a slightly higher temperature and narrowed as DHPE became the predominant lipid. With 90 mol % DHPE a broad, low-enthalpy transition was observed at a temperature of 88 °C, possibly representing the liquid-crystalline to inverted hexagonal ( $L_\alpha \rightarrow H_{II}$ ) phase transition. At 93 mol % DHPE, this transition was not clearly visible in the temperature range examined, but pure DHPE exhibited the  $L_\alpha \rightarrow H_{II}$  transition at 88 °C. The complex DSC behavior of DHPC/DHPE mixtures provides strong evidence for lipid phase separation phenomena. The onset and completion temperatures corresponding to the solidus and fluidus in a phase-separating system are plotted in Figure 2. The enthalpy of the main transition was calculated for each lipid mixture and found not to vary significantly with lipid composition (data not shown). DHPE/DHPC mixtures were also run on an MC-2 high-sensitivity calorimeter at a slower scan rate, 1.5 °C/min. In mixtures of intermediate composition, the onset and completion temperatures agreed well with those derived from the DSC-7 data. For example, at 48 mol % DHPE, the onset and completion temperatures recorded on the MC-2 were 42 (44 °C on the DSC-7) and 65 °C (64 °C on the DSC-7), respectively. However, the MC-2 data did show evidence of a pretransition at ~33 °C up to 23 mol % DHPE.

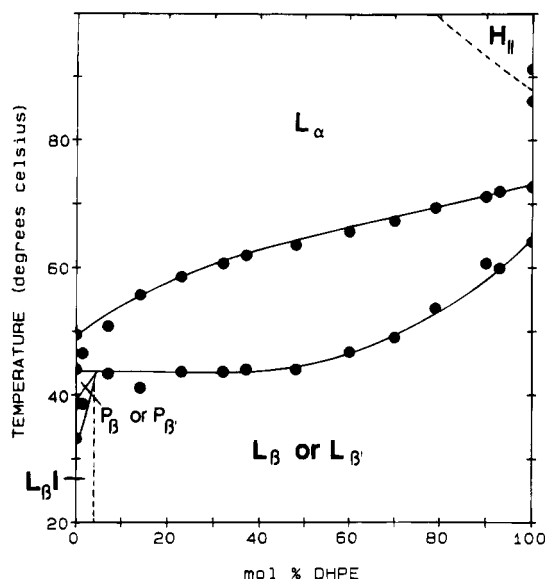


FIGURE 2: Proposed phase diagram of the fully hydrated DHPE/DHPC system as deduced from DSC and X-ray diffraction data. The initial (onset) and final (completion) temperatures (closed circles) are derived from the DSC curves shown in Figure 1. The  $L_{\beta}I$  phase exists only in the gel phase at low levels of DHPE. DHPE quickly converts the bilayer to the  $L_{\beta}$  or  $L_{\beta}'$  phase. The dashed line (upper right) indicates schematically that the addition of DHPC raises the temperature of (or removes) the  $L_{\alpha} \rightarrow H_{II}$  phase transition of DHPE.

**X-ray Diffraction of Fully Hydrated DHPE/DHPC Mixtures.** Representative X-ray diffraction patterns of fully hydrated DHPE/DHPC lipid mixtures at temperatures both below and above the main transition are shown in Figure 3, and the  $d$ -spacings of various DHPE/DHPC mixtures at temperatures both below and above the main phase transition temperature are plotted in Figure 4. At 25 °C, a sharp symmetric reflection was seen at  $1/4.07 \text{ \AA}^{-1}$  for DHPC in 70 wt %  $H_2O$  (Figure 3F), which is indicative of rigid hydrocarbon chains. The low-angle region displayed a lamellar diffraction pattern with a bilayer repeat distance  $d = 47.1 \text{ \AA}$  (Figures 3F and 4). This diffraction pattern exhibits a  $d$ -spacing that is much smaller than that of the corresponding ester-linked lipid, DPPC ( $d = 64 \text{ \AA}$ ), and indicates the presence of a gel phase interdigitated bilayer,  $L_{\beta}I$  (Ruocco et al., 1985; Kim et al., 1987a; Laggner et al., 1987). At 50 °C (Figure 3A), the sharp reflection at  $1/4.07 \text{ \AA}^{-1}$  was replaced by a broad, diffuse band centered at  $1/4.5 \text{ \AA}^{-1}$ . A lamellar diffraction pattern was still observed in the low-angle region (Figure 3A), but with a significantly increased bilayer repeat distance,  $d = 62.7 \text{ \AA}$  (Figure 4). Therefore, above the main transition, at 50 °C, DHPC is in a non-interdigitated, liquid-crystalline state ( $L_{\alpha}$ ).

Addition of 1.4 mol % DHPE to DHPC produced little change in the diffraction pattern at 25 °C. A sharp reflection was observed at  $1/4.07 \text{ \AA}^{-1}$ , and the bilayer repeat was measured to be  $d = 48.5 \text{ \AA}$  (Figure 4). This indicated that the lipid mixture was still in the  $L_{\beta}I$  phase at this concentration of DHPE. With greater amounts of DHPE in DHPC, however, differences in both the low- and wide-angle regions of the diffraction pattern at 25 °C were observed. At 7 mol % DHPE, a lamellar diffraction pattern was seen, but with a much increased bilayer repeat,  $d = 67.8 \text{ \AA}$  (Figure 4); a wide-angle reflection at  $1/4.18 \text{ \AA}^{-1}$  was observed. In comparison to the wide-angle reflection seen in pure DHPC,

this reflection appeared slightly broader. This was interpreted to mean that the bilayer had converted to a non-interdigitated lamellar gel form ( $L_{\beta}$  or  $L_{\beta}'$ ), hence the markedly increased bilayer repeat distance and the broader wide-angle band, reflecting the less ordered packing of the hydrocarbon chains in this phase than in the  $L_{\beta}I$  phase. The diffraction patterns of the lipid mixtures differed little from 14 mol % DHPE to 79 mol % DHPE for the lipid mixtures at 25 °C (Figure 3G–I). The bilayer repeat varied insignificantly between 67 and 69 Å (Figure 4) and a wide-angle reflection at approximately  $1/4.2 \text{ \AA}^{-1}$  was continually observed, showing that the mixtures had rigid hydrocarbon chains and were in the gel state at this temperature. At 93 mol % DHPE, the  $d$ -spacing decreased to 66.5 Å at 25 °C (Figure 4), while at the same temperature for 100 mol % DHPE (Figure 3J) the  $d$ -spacing decreased further to 61.3 Å (Figure 4). Above the transition temperature, at 70 °C, all of the lipid mixtures displayed a lamellar diffraction pattern and a diffuse band centered at approximately  $1/4.5$ – $1/4.6 \text{ \AA}^{-1}$  (Figure 3A–E), which indicated that the DHPE/DHPC mixtures were in the  $L_{\alpha}$  phase at this temperature. The bilayer repeat distance, however, showed greater variation with composition than in the gel phase (Figure 4). The  $d$ -spacing stayed relatively constant from 0 to 48 mol % DHPE at 70 °C,  $d = 62$ – $63 \text{ \AA}$ . Then, with increasing DHPE content, the measured  $d$ -spacing at 70 °C decreased steadily to a value of  $d = 51.7 \text{ \AA}$  for pure DHPE (Figure 4). At 95 °C, DHPE exhibited a diffraction pattern corresponding to a hexagonal  $H_{II}$  phase,  $d = 57 \text{ \AA}$  (Figure 4).

The electron density profiles of selected mixtures at 25 °C are displayed in Figure 5 and confirm the phase assignments made previously. The profiles were calculated using the phase sequence of  $h = 1-4$  ( $-,-,+,-$ ), which was found to be appropriate for DHPC (Kim et al., 1987a), except for pure DHPE for which the phase sequence ( $-,+,-,-$ ) was used (Hing et al., 1991). The assigned phase sequences were found to give satisfactory results for these mixtures. The profiles in Figure 5 show that the bilayer is interdigitated at low levels of DHPE in DHPC. The lipid layer thickness, as defined by the interbilayer phosphate peak separation ( $d_{p-p}$ ), is 31 Å. In addition, there is a significant amount of density in the center of the bilayer where the hydrocarbon chains overlap each other. At 23 mol % DHPE and above, however, the bilayer is clearly non-interdigitated. The bilayer thickness is much increased ( $d_{p-p} = 49 \text{ \AA}$ ) and a trough is visible in the center of the bilayer, indicating the presence of the terminal methyl groups of the hydrocarbon chains. Furthermore, the lipid layer thickness remains relatively constant as the DHPE composition is varied. This shows that variations in the  $d$ -spacing of the lipid in either the interdigitated or non-interdigitated state are mainly due to changes in the water layer thickness and, thus, are a reflection of the hydration of the various mixtures.

## DISCUSSION

We have examined fully hydrated mixtures of DHPC and DHPE, two ether-linked lipids that are capable of forming unusual phases in aqueous solution. DHPC forms a chain-interdigitated bilayer,  $L_{\beta}I$ , above approximately 30 wt %  $H_2O$  (Kim et al., 1987a; Laggner et al., 1987). DHPE, in contrast, forms the inverted hexagonal phase  $H_{II}$  at elevated temperatures (Boggs et al., 1981; Harlos & Eibl, 1981; Marsh & Seddon, 1982). The ester-linked counterpart of DHPC,

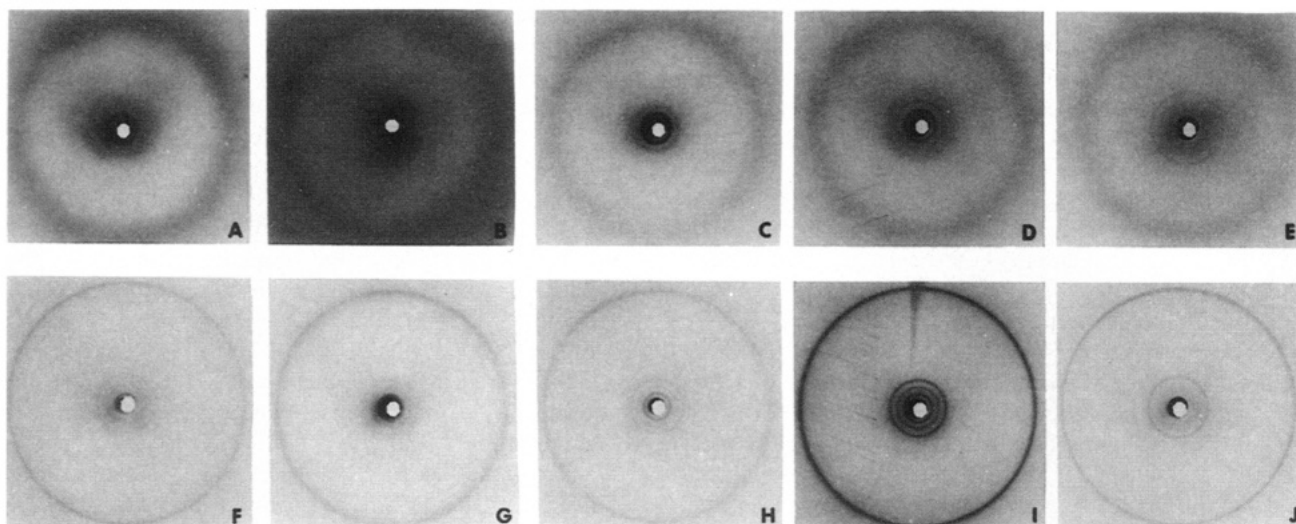


FIGURE 3: Representative X-ray diffraction patterns of fully hydrated DHPE/DHPC mixtures below (F–J,  $T = 25\text{ }^{\circ}\text{C}$ ) and above (A–E,  $T = 70\text{ }^{\circ}\text{C}$ ) the chain-melting transition temperature: (A, F) 0, (B, G) 14, (C, H) 48, (D, I) 79, and (E, J) 100 mol % DHPE.

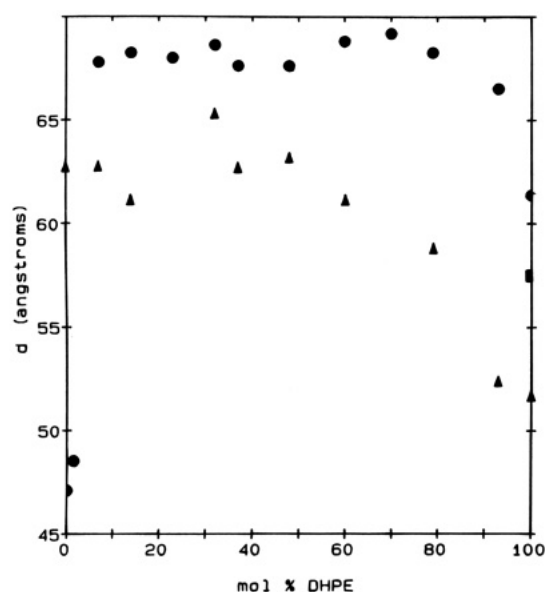


FIGURE 4: Bilayer periodicity of fully hydrated mixtures of DHPE and DHPC as a function of DHPE content, below ( $\bullet$ ,  $25\text{ }^{\circ}\text{C}$ ) and above ( $\blacktriangle$ ,  $70\text{ }^{\circ}\text{C}$ ) the chain-melting transition temperature, except for pure DHPC which was measured at  $50\text{ }^{\circ}\text{C}$ . The hexagonal phase of DHPE was observed at  $95\text{ }^{\circ}\text{C}$  ( $\blacksquare$ ).

DPPC, does not form the  $L_{\beta}I$  phase under normal conditions of pressure and hydration, but can be induced to interdigitate under certain conditions (McIntosh et al., 1983; Braganza & Worcester, 1986). However, chain interdigitation does occur to a significant extent in mixtures of DHPC and DPPC. DPPC can be accommodated up to 30 mol % in an interdigitated bilayer of DHPC before the lipid converts to a non-interdigitated form (Kim et al., 1987b; Lohner et al., 1987). In a similar study of mixtures of DHPE and its ester-linked counterpart, DPPE, it was found that DPPE destabilized the  $H_{II}$  phase of DHPE relative to its  $L_{\alpha}$  phase, so that it formed at higher than normal temperatures (Hing et al., 1991).

DHPC, and not DPPC, is thought to form the  $L_{\beta}I$  phase under normal conditions because of the absence of two carbonyl bonds from the ether linkages that are present in the ester bonds of DPPC. A combination of hydration effects at the polar group and the increased area of the head group relative to the hydrocarbon chains are believed to contribute

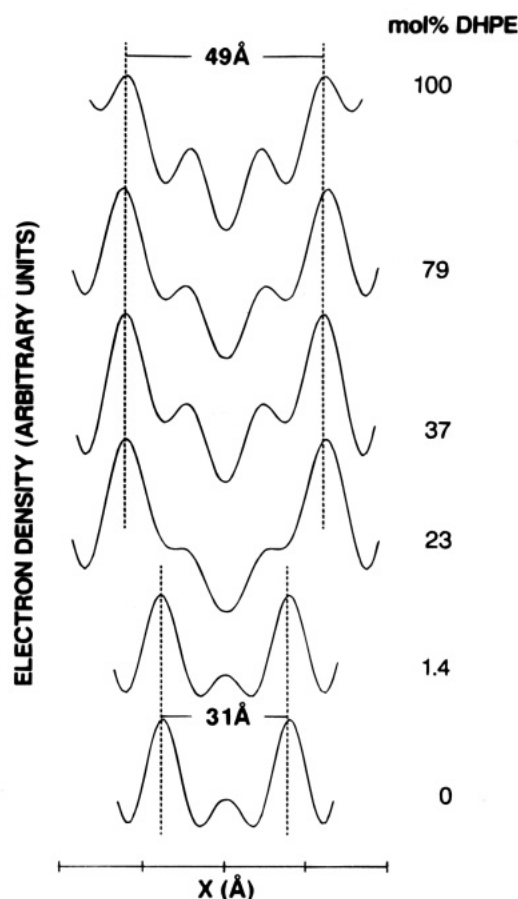


FIGURE 5: Electron density profiles of representative mixtures of DHPE and DHPC in the gel phase ( $T = 25\text{ }^{\circ}\text{C}$ ). Bilayers are interdigitated at very low levels of DHPE and non-interdigitated at all other compositions. The bilayer thickness stays approximately constant in each phase.

to the formation of this phase. In this study, we have found that the addition of 7 mol % DHPE to an interdigitated bilayer of DHPC converts it to a non-interdigitated bilayer. It is proposed that this happens because of the relatively smaller head group of DHPE. The head groups therefore are packed closer together than in a bilayer containing just PC molecules, and chain interdigitation cannot occur without exposing the terminal methyl groups to water.

The packing requirements of the lipid molecules in an interdigitated bilayer appear to be fairly demanding. Simionovitch et al. (1987) found that, at 50 mol % cholesterol in DHPC, the bilayer was non-interdigitated as determined by X-ray diffraction and  $^2\text{H}$  NMR. However, a more detailed study of the effect of cholesterol suggests that DHPE is accommodated slightly more readily than cholesterol in the  $L_{\beta}\text{I}$  phase of DHPC since, at as low as 0.1 mol % cholesterol in DHPC, Laggner et al. (1991) saw signs of non-interdigitation by X-ray diffraction. Furthermore, complete conversion of DHPC to a non-interdigitated bilayer phase occurred by 5 mol % cholesterol. At 1.4 mol % DHPE in DHPC, we observed only the  $L_{\beta}\text{I}$  phase; however, conversion to a non-interdigitated ( $L_{\beta}$  or  $L_{\beta}'$ ) bilayer phase occurred by 7 mol % DHPE. Therefore, cholesterol appears to be slightly more effective at inducing an interdigitated to non-interdigitated transition in DHPC than is DHPE. This is understandable since cholesterol partitions mainly into the hydrophobic region of the bilayer, while DHPE makes contributions to both the head group area and the hydrocarbon chain region. Therefore, the mismatch in cross-sectional area between the polar and nonpolar regions is alleviated more quickly in the case of cholesterol, thereby favoring the non-interdigitated state. Others have found interdigitated bilayers to be much more tolerant of sterols, up to 27 mol % in the  $L_{\beta}\text{I}$  phase (Komatsu & Rowe, 1991; Kao et al., 1990). However, these studies differed in the conditions and types of lipids and so cannot be readily compared.

The  $H_{\text{II}}$  phase in PE is thought to arise from nearly the opposite conditions that give rise to the  $L_{\beta}\text{I}$  phase. In this case, because of the tighter packing of the ethanolamine head groups and a relatively large volume of hydrophobic region, PEs have high intrinsic curvature (Gruner, 1985), and the  $H_{\text{II}}$  phase becomes more favored (Shipley, 1973; Boggs et al., 1981; Seddon et al., 1983). For this reason, DHPE forms the  $H_{\text{II}}$  phase at much lower temperatures than its ester-linked counterpart, DPPC (Hing et al., 1991). The absence of the carbonyl oxygens in DHPE allows the polar head groups of DHPE to pack closer together than in DPPC. We have added to DHPE a lipid with a relatively large head group relative to the cross-sectional area of its chain region (DHPC). In this manner, we have lessened the mismatch in cross-sectional areas between the polar and nonpolar regions of DHPE and, thus, destabilized the  $H_{\text{II}}$  phase with respect to the  $L_{\alpha}$  phase. The bilayer-stabilizing effect of PCs added to PEs has been demonstrated previously. Silvius (1986) found that the addition of dimyristoylphosphatidylcholine to dimyristoylphosphatidylethanolamine could raise the temperature of the  $L_{\alpha} \rightarrow H_{\text{II}}$  phase transition by up to 30 °C. Lohner et al. (1991) obtained similar results by adding 1-palmitoyl-2-oleoylphosphatidylcholine to ethanolamine plasmalogen. While the DSC data at high temperatures in the range 90–100 mol % DHPE are inconsistent (see Figure 2), it is clear that the addition of ~10 mol % DHPC is sufficient to elevate (to >100 °C) and/or remove the  $L_{\alpha} \rightarrow H_{\text{II}}$  transition.

Binary mixtures of DHPE/DHPC show complex DSC heating curves indicative of phase separation in the gel phase but phospholipid miscibility in the melted-chain phase (Figures 1 and 2). The addition of small amounts of DHPE to DHPC appears to abolish the pretransition, as shown by thermograms recorded on the DSC-7; however, heating scans performed at a slower scan rate on the Microcal-2 could

detect the pretransition in these mixtures up to about 23 mol % DHPE (data not shown). The pretransition is not resolved well enough in our DSC-7 heating scans to plot this transition temperature accurately on the phase diagram. The analogy to existing binary phase diagrams of ester-linked PE/PC mixtures is complicated by the existence of the  $L_{\beta}\text{I}$  phase at very low levels of DHPE. The DSC data (Figure 1) and the plot of the onset and completion temperatures (Figure 2) provide strong evidence for gel phase immiscibility/phase separation, as has been suggested by several previous studies (Arnold et al., 1981; Blume & Ackermann, 1974; Luna & McConnell, 1978; Mendelsohn & Koch, 1980; Blume et al., 1982). However, X-ray diffraction of DHPE/DHPC mixtures showed only a single bilayer periodicity for the gel phase at all compositions. In view of the DSC data, it is possible that two phase-separated gel phases with essentially identical bilayer periodicities are present. In contrast, DHPC and DHPE appear to be fully miscible in the melted-chain  $L_{\alpha}$  phase. Between the onset (solidus) and completion (fluidus) temperatures, bilayer gel and bilayer fluid  $L_{\alpha}$  phases coexist.

An unexpected result is the dependence of the bilayer periodicity as a function of DHPE content (Figure 4). The small  $d$ -spacing of 47 Å observed for the  $L_{\beta}\text{I}$  gel phase of DHPC quickly converts to a large  $d$ -spacing of 68 Å upon the addition of as little as 7 mol % DHPE. This is larger than the  $d$ -spacing of DPPC (64 Å), which is non-interdigitated (Janiak et al., 1976; Inoko & Mitsui, 1978). Upon continued addition of DHPE, the  $d$ -spacing surprisingly remains approximately constant at 68 Å up to about 79 mol % DHPE before decreasing to 62 Å for pure DHPE. Since DHPC is hydrated to a greater extent than DHPE, one might have expected a continuous decrease in the  $d$ -spacing as the amount of DHPE increases. According to the X-ray diffraction evidence, however, the hydration effects of the PC predominate even at relatively high PE levels. The electron density profiles calculated for the lipid mixtures confirm this conclusion by showing that the bilayer thickness remains approximately the same in each phase; therefore, the observed changes in  $d$ -spacing are due to changes in the thickness of the water layer. In the liquid-crystalline phase, the  $d$ -spacing seems more responsive to the level of DHPE than in the gel phase. This may reflect greater miscibility of the two lipids in the fluid phase.

In summary, our experiments demonstrate that a small amount of DHPE can abolish the  $L_{\beta}\text{I}$  phase of DHPC and, conversely, that a similarly small amount of DHPC significantly compromises the  $H_{\text{II}}$  phase-forming ability of DHPE. In addition, it was found that, in mixtures of DHPE and DHPC, DHPC is the phospholipid that predominantly determines the hydration state of the bilayer. At low temperatures, the DSC data provide evidence for gel phase immiscibility, presumably of PC- and PE-rich gel phases, whereas complete miscibility is observed in the fluid, melted-chain bilayer phase. It has been suggested that a function of sterols in cell membranes is to prevent chain interdigitation (Kao et al., 1990; Lohner et al., 1991). These results show that another lipid, a phosphatidylethanolamine, can prevent chain interdigitation, and it is likely that other membrane components have this ability as well. Furthermore, the lamellar liquid-crystalline phase is stabilized relative to the inverted hexagonal phase in lipid mixtures. Since cell membranes usually are complex mixtures of lipids and proteins rather than a single lipid species, these results

question the occurrence of the  $L_{\beta}I$  and  $H_{II}$  phases in nature, and at the very least place strict constraints on the conditions for the formation of these phases in natural systems.

## REFERENCES

- Arnold, K., Losche, A., & Gawrisch, K. (1981) *Biochim. Biophys. Acta* 645, 143–148.
- Blume, A., & Ackermann, T. (1974) *FEBS Lett.* 43, 71–74.
- Blume, A., Wittebort, R. J., Das Gupta, S. K., & Griffin, R. G. (1982) *Biochemistry* 21, 6243–6253.
- Boggs, J. M., Stamp, D., Hughes, D. W., & Deber, C. M. (1981) *Biochemistry* 20, 5728–5735.
- Braganza, L. F., & Worcester, D. L. (1986) *Biochemistry* 25, 2591–2596.
- Chapman, D., Byrne, P., & Shipley, G. G. (1966) *Proc. R. Soc. London A290*, 115–142.
- Elliott, A. J. (1965) *J. Sci. Instrum.* 42, 312–316.
- Franks, A. (1958) *Br. J. Appl. Phys.* 9, 349–352.
- Goldfine, H., Johnston, N. C., Mattai, J., & Shipley, G. G. (1987) *Biochemistry* 26, 2814–2822.
- Gruner, S. M. (1985) *Proc. Natl. Acad. Sci. U.S.A.* 82, 3665–3669.
- Haas, N. S., Sripada, P. K., & Shipley, G. G. (1990) *Biophys. J.* 57, 117–124.
- Harlos, K., & Eibl, H. (1981) *Biochemistry* 20, 2888–2892.
- Hauser, H., Paltauf, F., & Shipley, G. G. (1982) *Biochemistry* 21, 1061–1067.
- Hing, F. S., Maulik, P. R., & Shipley, G. G. (1991) *Biochemistry* 30, 9007–9015.
- Hitchcock, P. B., Mason, R., Thomas, K. M., & Shipley, G. G. (1974) *Proc. Natl. Acad. Sci. U.S.A.* 71, 3036–3040.
- Inoko, Y., & Mitsui, T. (1978) *J. Phys. Soc. Jpn.* 44, 1918–1924.
- Israelachvili, J. N., Marcelja, S., & Horn, R. G. (1980) *Q. Rev. Biophys.* 13, 121–200.
- Janiak, M. J., Small, D. M., & Shipley, G. G. (1976) *Biochemistry* 15, 4575–4580.
- Janiak, M. J., Small, D. M., & Shipley, G. G. (1979) *J. Biol. Chem.* 254, 6068–6078.
- Kao, Y. L., Chong, P. L., & Huang, C. (1990) *Biochemistry* 29, 1315–1322.
- Kim, J. T., Mattai, J., & Shipley, G. G. (1987a) *Biochemistry* 26, 6592–6598.
- Kim, J. T., Mattai, J., & Shipley, G. G. (1987b) *Biochemistry* 26, 6599–6603.
- Komatsu, H., & Rowe, E. S. (1991) *Biochemistry* 30, 2463–2470.
- Laggner, P., Lohner, K., Degovics, G., Muller, K., & Schuster, A. (1987) *Chem. Phys. Lipids* 44, 31–60.
- Laggner, P., Lohner, K., Koynova, R., & Tenchov, B. (1991) *Chem. Phys. Lipids* 60, 153–161.
- Lohner, K., Schuster, A., Degovics, G., Muller, K., & Laggner, P. (1987) *Chem. Phys. Lipids* 44, 61–70.
- Lohner, K., Balgavy, P., Hermetter, A., Paltauf, F., & Laggner, P. (1991) *Biochim. Biophys. Acta* 1061, 132–140.
- Luna, E. J., & McConnell, H. M. (1978) *Biochim. Biophys. Acta* 509, 462–473.
- Marsh, D., & Seddon, J. M. (1982) *Biochim. Biophys. Acta* 690, 117–123.
- Mattai, J., Sripada, P. K., & Shipley, G. G. (1987) *Biochemistry* 26, 3287–3297.
- McIntosh, T. J., McDaniel, R. V., & Simon, S. A. (1983) *Biochim. Biophys. Acta* 731, 109–114.
- Mendelsohn, R., & Koch, C. C. (1980) *Biochim. Biophys. Acta* 598, 260–271.
- Mulukutla, S., & Shipley, G. G. (1984) *Biochemistry* 23, 2514–2519.
- Ruocco, M. J., & Shipley, G. G. (1982a) *Biochim. Biophys. Acta* 691, 309–320.
- Ruocco, M. J., & Shipley, G. G. (1982b) *Biochim. Biophys. Acta* 684, 59–66.
- Ruocco, M. J., Siminovitch, D. J., & Griffin, R. G. (1985) *Biochemistry* 24, 2406–2411.
- Seddon, J. M., Cevc, G., & Marsh, D. (1983) *Biochemistry* 22, 1280–1289.
- Shah, J., Sripada, P. K., & Shipley, G. G. (1990) *Biochemistry* 29, 4254–4262.
- Shah, J., Duclos, R. I., & Shipley, G. G. (1994) *Biophys. J.* 66, 1469–1478.
- Shipley, G. G. (1973) in *Biological Membranes* (Chapman, D., & Wallach, D. F. H., Eds.) Vol. 2, pp 1–89, Academic Press, London.
- Silvius, J. R. (1986) *Biochim. Biophys. Acta* 857, 217–228.
- Siminovitch, D. J., Ruocco, M. J., Makriyannis, A., & Griffin, R. G. (1987) *Biochim. Biophys. Acta* 901, 191–200.
- Snyder, F. (1991) in *Biochemistry of Lipids, Lipoproteins and Membranes* (Vance, D. E., & Vance, J. E., Eds.) pp 241–267, Elsevier, Amsterdam.
- Wieslander, A., Christiansson, A., Rilfors, L., & Lindblom, G. (1980) *Biochemistry* 19, 3650–3655.
- Wieslander, A., Christiansson, A., Rilfors, L., Khan, A., Johansson, L. B.-A., & Lindblom, G. (1981a) *FEBS Lett.* 124, 273–278.
- Wieslander, A., Rilfors, L., Johansson, L. B.-A., & Lindblom, G. (1981b) *Biochemistry* 20, 730–735.

BI9503357